

SOLAR-LIKE OSCILLATIONS IN THE METAL-POOR SUBGIANT ν INDI: CONSTRAINING THE MASS AND AGE USING ASTEROSEISMOLOGY

TIMOTHY R. BEDDING,¹ R. PAUL BUTLER,² FABIEN CARRIER,³ FRANCOIS BOUCHY,^{3,4}
 BRENDON J. BREWER,¹ PATRICK EGGENBERGER,³ FRANK GRUNDAHL,⁵ HANS KJELDSSEN,⁵
 CHRIS MCCARTHY,² TINE BJØRN NIELSEN,⁵ ALON RETTER,^{1,6} CHRISTOPHER G. TINNEY⁷
To appear in ApJ

ABSTRACT

Asteroseismology is a powerful method for determining fundamental properties of stars. We report the first application to a metal-poor object, namely the subgiant star ν Ind. We measured precise velocities from two sites, allowing us to detect oscillations and infer a large frequency separation of $\Delta\nu = 24.25 \pm 0.25 \mu\text{Hz}$. Combining this value with the location of the star in the H-R diagram and comparing with standard evolutionary models, we were able to place constraints on the stellar parameters. In particular, our results indicate that ν Ind has a low mass ($0.85 \pm 0.04 M_{\odot}$) and is at least 9 Gyr old.

Subject headings: stars: individual (ν Ind) — stars: oscillations — Sun: helioseismology

1. INTRODUCTION

Asteroseismology is a powerful method for determining fundamental properties of stars. This is because oscillation frequencies give strong constraints on the internal structure that are independent of classical observations. Observations of solar-like oscillations are accumulating rapidly, and measurements have recently been reported for several main-sequence and subgiant stars, including α Cen A (Bouchy & Carrier 2002; Bedding et al. 2004), α Cen B (Carrier & Bourban 2003; Kjeldsen et al. 2005), β Vir (Martic et al. 2004; Carrier et al. 2005b), μ Ara (Bouchy et al. 2005), HD 49933 (Mosser et al. 2005) and η Boo (Kjeldsen et al. 2003; Carrier et al. 2005a; Guenther et al. 2005). All of these stars have solar metallicity or greater. Asteroseismology is particularly useful for constraining the evolutionary status of stars with low metallicity (e.g. D’Antona et al. 2005). Here, we report the first oscillation measurements of a metal-poor star.

We have observed the subgiant ν Ind (HR 8515; HD 211998; HIP 110618), whose iron abundance is only 3% of solar. We adopt the following stellar parameters: $V = 5.28$, $T_{\text{eff}} = 5300 \pm 100$ K, $L = 6.2 L_{\odot}$ and $[\text{Fe}/\text{H}] = -1.4 \pm 0.1$ (Nissen et al. 1997; Gratton et al. 2000). Note that the Bright Star Catalogue (Hoffleit 1982) incorrectly lists this star as a binary with spectral types A3V:+F9V. In fact, ν Ind is a single star with spectral type G0 (Lambert & McWilliam 1986).

2. VELOCITY OBSERVATIONS AND POWER SPECTRA

We observed ν Ind in August 2002 from two sites. At Sid- ing Spring Observatory in Australia we used UCLES (University College London Echelle Spectrograph) with the 3.9-m Anglo-Australian Telescope (AAT). An iodine absorption cell was used to provide a stable wavelength reference, with the same setup that we have previously used with this spectrograph

(Butler et al. 2004). At the European Southern Observatory on La Silla in Chile we used the CORALIE spectrograph with the 1.2-m Swiss telescope. A thorium emission lamp was used to provide a stable wavelength reference, and the velocities were processed using the method described by Bouchy et al. (2001).

With UCLES we obtained 680 spectra of ν Ind, with typical exposure times of 300 s (but sometimes as short as 200 s in the best conditions) and a dead time between exposures of 61 s. With CORALIE we obtained 521 spectra, with typical exposure times of 360 s and a dead time between exposures of 128 s.

The resulting velocities, with nightly means subtracted, are shown in Fig. 1. As can be seen, the weather was good in Australia but poor in Chile (we were allocated seven nights with UCLES and 14 with CORALIE).

Most of the scatter in the velocities, especially for UCLES, is due to oscillations. Figure 2 shows a close-up of the first night. Oscillations with a period of about 50 min and variable amplitude (due to beating between modes) are visible here and throughout the time series. We also see good agreement between the two instruments, within measurement uncertainties, during the overlap (although we should note that the difference in absolute velocities is not known and has been adjusted to give the best fit).

Our analysis of these velocities follows the method that we developed for α Cen A (Butler et al. 2004) and α Cen B (Kjeldsen et al. 2005). We have used the measurement uncertainties, σ_i , as weights in calculating the power spectrum (according to $w_i = 1/\sigma_i^2$), but modified some of the weights to account for a small fraction of bad data points. In this case, 4 data points from UCLES and 24 from CORALIE needed to be down-weighted. The power spectra of the individual time series and of the combination are shown in Fig. 3. The differences between the three panels can be attributed to the effects of beating between modes.

¹ School of Physics A28, University of Sydney, NSW 2006, Australia; bedding@physics.usyd.edu.au; brewer@physics.usyd.edu.au

² Carnegie Institution of Washington, Department of Terrestrial Magnetism, 5241 Broad Branch Road NW, Washington, DC 20015-1305; paul@dtm.ciw.edu, chris@dtm.ciw.edu

³ Observatoire de Genève, Ch. des Maillettes 51, CH-1290 Sauverny, Switzerland; fabien.carrier@obs.unige.ch; francois.bouchy@obs.unige.ch; patrick.eggenberger@obs.unige.ch

⁴ Laboratoire d’Astrophysique de Marseille, Traverse du Siphon, BP 8, 13376 Marseille Cedex 12, France

⁵ Department of Physics and Astronomy, University of Aarhus, DK-8000 Aarhus C, Denmark; hans@phys.au.dk, fgj@phys.au.dk, tbn@phys.au.dk

⁶ Department of Astronomy and Astrophysics, Pennsylvania State University, 525 Davey Lab, University Park, PA 16802-6305; retter@astro.psu.edu

⁷ Anglo-Australian Observatory, P.O. Box 296, Epping, NSW 1710, Australia; cgt@aaopep.aao.gov.au

The low metallicity of ν Ind means that the lines in its spectrum are fewer and weaker than for stars of solar metallicity. This, together with its relative faintness ($V = 5.3$), means that the Doppler precision for ν Ind is poorer than for other stars observed with the same instruments, such as α Cen A and B. We measured the average noise in the amplitude spectrum of ν Ind at frequencies above the stellar signal (0.6–1 mHz) to be 17.3 cm s^{-1} for UCLES, 27.2 cm s^{-1} for CORALIE and 14.9 cm s^{-1} for the combined data. Using these values, we calculated the noise per minute of observing time to be 5.9 m s^{-1} for UCLES and 9.5 m s^{-1} for CORALIE, where the difference is due to a combination of factors, primarily the telescope aperture but also including spectrograph design, sky conditions and observing duty cycle.

The inset in each panel of Fig. 3 shows the spectral window (the response to a single pure sinusoid). For the single-site data we see sidelobes at $\pm 11.6 \mu\text{Hz}$ that are very strong (51% in power for UCLES and 57% for CORALIE). These are due to daytime gaps in the observing window. When the data are combined, the sidelobes are drastically reduced (to 16% in power) and are also slightly shifted, occurring at $\pm 10.8 \mu\text{Hz}$. In the cases of α Cen A and B, we generated power spectra in which the weights were adjusted on a night-by-night basis in order to minimize the sidelobes. We have not done that for ν Ind because the sidelobes for the two-site data are already quite low.

3. LARGE FREQUENCY SEPARATION

Mode frequencies for low-degree p-mode oscillations are approximated reasonably well by a regular series of peaks:

$$\nu_{n,l} = \Delta\nu(n + \frac{1}{2}l + \epsilon) - l(l+1)D_0. \quad (1)$$

Here n (the radial order) and l (the angular degree) are integers, $\Delta\nu$ (the large separation) depends on the sound travel time across the whole star, D_0 is sensitive to the sound speed near the core and ϵ is sensitive to the surface layers. See Christensen-Dalsgaard (2004) for a recent review of the theory of solar-like oscillations.

The large separation, $\Delta\nu$, is proportional to the square root of the mean density of the star. Scaling from the Sun, for which $\Delta\nu = 135 \mu\text{Hz}$, we expect ν Ind to have a large separation of about $25 \mu\text{Hz}$. In order to search for a regular series of peaks from which to measure the large separation, we calculated the autocorrelation function of the power spectrum. The result is shown in Fig. 4 and the peak at $10.8 \mu\text{Hz}$ (dashed line) is the main sidelobe caused by the daily gaps (see above). We interpret the peak at $24.5 \mu\text{Hz}$ as due to the large separation, with smaller peaks at $\pm 10.8 \mu\text{Hz}$ from this being due to daily aliases (the peak at $13 \mu\text{Hz}$ also coincides with half the large separation). The peak at $5 \mu\text{Hz}$ is not easily explained by the regular p-mode structure and may reflect departures of a few modes from the asymptotic relation in equation 1.

As a check of this result, we also measured the large separation directly from the light curve data using Bayesian methods (see Gregory 2005 for a good introduction to Bayesian analysis). We modelled the light curve as a sum of sinusoids, where the number of sinusoids, together with their amplitudes, phases and frequencies, were treated as unknowns. An advantage of this approach is that the amplitudes and phases can be integrated out of the problem at the beginning (Bretthorst 1988), so that we only need to fit the frequencies and their number. To determine the large separation, we chose the prior distribution for the frequencies to be periodic, with period $\frac{1}{2}\Delta\nu$ (considered unknown). We fixed the central frequency of this periodic comb

to be the highest peak in the power spectrum ($313.14 \mu\text{Hz}$). We then calculated the posterior distribution for $\Delta\nu$, which is shown in the lower panel of Fig. 4. There is a single strong peak with a value of $\Delta\nu = 24.25 \pm 0.25 \mu\text{Hz}$, in agreement with the peak of the autocorrelation. More details of this method, which is similar to the approach used by Bretthorst (2003) and appears to be very promising for this type of analysis, will be presented separately (B. Brewer et al., in prep.).

4. CONSTRAINTS ON THE STELLAR PARAMETERS

What can we learn about ν Ind from our measurement of $\Delta\nu$? Figure 5 shows the location of the star in the H-R diagram, together with some theoretical evolutionary tracks. The box, which is the same in each panel, shows the observed position of ν Ind from classical measurements. The value for T_{eff} ($5300 \pm 100 \text{ K}$) is the mean of published photometric estimates (Nissen et al. 1997; Gratton et al. 2000), where we note the large uncertainty in the effective temperature scale for metal-poor stars. The luminosity is based on the Hipparcos parallax ($34.6 \pm 0.6 \text{ mas}$), with bolometric corrections from Alonso et al. (1999). Note that the bolometric correction is a function of effective temperature, hence the slope of the box. The diagonal dashed lines, which are also the same in each panel, are loci of constant radius, calculated from $L \propto R^2 T_{\text{eff}}^4$. We can immediately see that a measurement of the radius from interferometry would be valuable in constraining the location of the star in the H-R diagram, as has already been shown for other stars (Kervella et al. 2003; Pijpers et al. 2003; Kervella et al. 2004; Thévenin et al. 2005).

The curved lines in Fig. 5 are evolutionary tracks for a range of masses, using model calculations similar to those by Christensen-Dalsgaard (1982). We used a metallicity of $Z = 0.001$ (with hydrogen and helium mass fractions of $X = 0.75$ and $Y = 0.249$, respectively) and the three panels differ in the adopted value of the mixing-length parameter ($\alpha = 1.7, 1.8$ and 1.9), where the solar value is $\alpha_{\odot} = 1.83$. The relatively rapid evolution in this subgiant phase means each track can be described by a single age, as shown in the figure. Finally, the diagonal lines are contours of constant $\Delta\nu$. We calculated these from the evolutionary models by scaling from the Sun (since $\Delta\nu$ is proportional to the square root of the mean density).

We see that our measurement of $\Delta\nu$ significantly constrains the parameters of ν Ind. This is quantified in Fig. 6, in which the thin error bars show the range of each parameter based on classical measurements alone (L and T_{eff}), while the thick bars show the situation after we have added the constraint provided by our measurement of $\Delta\nu$. Including this constraint reduces the uncertainty in both effective temperature and radius, for a given value of α , by a factor of four.

What can we say about the mass of ν Ind? Even with no constraints from seismology, the requirement that ν Ind be younger than the universe (13.7 Gyr; Spergel et al. 2003) sets a lower limit of $0.81 M_{\odot}$. A star of lower mass would not have had time to evolve this far. Note that this limit, which we derived from the tracks in Fig. 6, is essentially independent of the mixing length. This is because the value of α has little effect on the fusion rate in the core, and hence on the time for a star of given mass to leave the main sequence and enter the subgiant phase. Meanwhile, an upper limit on the mass is obtained from our measurement of $\Delta\nu$, provided we also set a lower limit on α (third panel of Fig. 6). Adopting a plausible lower limit of $\alpha \geq 1.7$ gives an upper limit for the mass of $0.89 M_{\odot}$.

We can also set interesting limits on the age of ν Ind. From the bottom panel of Fig. 6, and again setting $\alpha > 1.7$ as a plausible limit, we see that the age must be at least 9 Gyr. This confirms that ν Ind is, indeed, very old and must have been formed very early in the history of the Galaxy. The final results of our analysis are summarized in Table 1, where we list our best estimates for the parameters of ν Ind, assuming that $Z = 0.001$ and $\alpha = 1.8 \pm 0.1$.

With the data currently available, what constraints can we set on the mixing length? The dashed line at an age of 13.7 Gyr in Fig. 6 indicates the upper limit set by age of the universe. This indicates that the mixing length cannot be greater than 2.1. We expect much stronger constraints on α , and also on the other stellar parameters, to come from the individual oscillation frequencies. The extraction of these frequencies and a comparison with theoretical models is deferred to a future paper (F. Carrier et al., in prep.). An accurate measurement of the radius using interferometry would also be extremely valuable.

5. OSCILLATION AMPLITUDE

The amplitudes of individual modes are affected by the stochastic nature of the excitation and by the (unknown) value of the mode lifetime. To measure the oscillation amplitude of ν Ind in a way that is independent of these effects, we have followed the method introduced by Kjeldsen et al. (2005). In brief, this involves the following steps: (i) smoothing the power spectrum heavily to produce a single hump of excess power that is insensitive to the fact that the oscillation spectrum has discrete peaks; (ii) converting to power density by multiplying by the effective length of the observing run (4.42 d, which we calculated from the area under the spectral window in power); (iii) fitting and subtracting the background noise; and (vi) multiplying by $\Delta\nu/3.0$ and taking the square root, in order to convert to amplitude per oscillation mode. For more details, see Kjeldsen et al. (2005).

The result is shown in Fig. 7. The peak amplitude per mode

is 0.95 ms^{-1} , which occurs at a frequency of $\nu_{\text{max}} = 320 \mu\text{Hz}$ (period 52 min). This value of ν_{max} is consistent with that expected from scaling the acoustic cutoff frequency of the Sun (Brown et al. 1991; Kjeldsen & Bedding 1995). The observed peak amplitude is 4.6 times the solar value, when the latter is measured using stellar techniques (Kjeldsen et al. 2005), which is substantially less than the value of 7.3 expected from the L/M scaling proposed by Kjeldsen & Bedding (1995) but is in good agreement with the $(L/M)^{0.7}$ scaling suggested for main-sequence stars by Samadi et al. (2005). A measurement of the mode lifetimes in ν Ind would be particularly useful.

6. CONCLUSIONS

We have observed solar-like oscillations in the metal-poor subgiant star ν Ind and measured the large frequency separation. We used this, together with the location of the star in the H-R diagram and standard evolutionary models, to place constraints on the stellar parameters. Our results, summarized in Table 1, confirm that ν Ind has a low mass and a large age and represent the first application of asteroseismology to a metal-poor star. Further constraints on the parameters, particularly the mixing length, should come from comparing individual oscillation frequencies with theoretical models.

We are extremely grateful to Conny Aerts for agreeing a time swap on CORALIE that allowed us to observe at the optimum time of year. We also thank Geoff Marcy for useful advice and enthusiastic support. This work was supported financially by the Australian Research Council, the Swiss National Science Foundation, the Danish Natural Science Research Council, the Danish National Research Foundation through its establishment of the Theoretical Astrophysics Center, and by a research associate fellowship from Penn State University. We further acknowledge support by NSF grant AST-9988087 (RPB) and by SUN Microsystems.

REFERENCES

- Alonso, A., Arribas, S., & Martínez-Roger, C., 1999, *A&AS*, 140, 261.
 Bedding, T. R., Kjeldsen, H., Butler, R. P., McCarthy, C., Marcy, G. W., O'Toole, S. J., Tinney, C. G., & Wright, J. T., 2004, *ApJ*, 614, 380.
 Bouchy, F., Bazot, M., Santos, N. C., Vauclair, S., & Sosnowska, D., 2005, *A&A*, 440, 609.
 Bouchy, F., & Carrier, F., 2002, *A&A*, 390, 205.
 Bouchy, F., Pepe, F., & Queloz, D., 2001, *A&A*, 374, 733.
 Brethorst, G. L., *Bayesian Spectrum Analysis and Parameter Estimation*, volume 48 of *Lecture Notes in Statistics*. Springer-Verlag: New York, 1988.
 Brethorst, G. L., 2003, In Willimas, C. J., editor, *AIP Conf. Proc.* 659: *Bayesian Inference and Maximum Entropy Methods in Science and Engineering*, page 3. available from <http://bayes.wustl.edu/>.
 Brown, T. M., Gilliland, R. L., Noyes, R. W., & Ramsey, L. W., 1991, *ApJ*, 368, 599.
 Butler, R. P., Bedding, T. R., Kjeldsen, H., McCarthy, C., O'Toole, S. J., Tinney, C. G., Marcy, G. W., & Wright, J. T., 2004, *ApJ*, 600, L75.
 Carrier, F., & Bourban, G., 2003, *A&A*, 406, L23.
 Carrier, F., Eggenberger, P., & Bouchy, F., 2005a, *A&A*, 434, 1085.
 Carrier, F., Eggenberger, P., D'Alessandro, A., & Weber, L., 2005b, *NewA*, 10, 315.
 Christensen-Dalsgaard, J., 1982, *MNRAS*, 199, 735.
 Christensen-Dalsgaard, J., 2004, *Sol. Phys.*, 220, 137.
 D'Antona, F., Cardini, D., Di Mauro, M. P., Maceroni, C., Mazzitelli, I., & Montalbán, J., 2005, *MNRAS*, 363, 847.
 Gratton, R. G., Sneden, C., Carretta, E., & Bragaglia, A., 2000, *A&A*, 354, 169.
 Gregory, P. C., *Bayesian Logical Data Analysis for the Physical Sciences*. Cambridge University Press, 2005.
 Guenther, D. B., Kallinger, T., Reegen, P., Weiss, W. W., Matthews, J. M., Kuschnig, R., Marchenko, S., Moffat, A. F. J., Rucinski, S. M., Sasselov, D., & Walker, G. A. H., 2005, *ApJ*, in press (arXiv:astro-ph/0503695).
 Hoffleit, D., *The Bright Star Catalogue*. Yale University Observatory, New Haven, 1982.
 Kervella, P., Thévenin, F., Morel, P., Berthomieu, G., Bordé, P., & Provost, J., 2004, *A&A*, 413, 251.
 Kervella, P., Thévenin, F., Ségransan, D., Berthomieu, G., Lopez, B., Morel, P., & Provost, J., 2003, *A&A*, 404, 1087.
 Kjeldsen, H., & Bedding, T. R., 1995, *A&A*, 293, 87.
 Kjeldsen, H., Bedding, T. R., Baldry, I. K., Bruntt, H., Butler, R. P., Fischer, D. A., Frandsen, S., Gates, E. L., Grundahl, F., Lang, K., Marcy, G. W., Misch, A., & Vogt, S. S., 2003, *AJ*, 126, 1483.
 Kjeldsen, H., Bedding, T. R., Butler, R. P., Christensen-Dalsgaard, J., Kiss, L., McCarthy, C., Marcy, G. W., Tinney, C. G., & Wright, J. T., 2005, *ApJ*, 635, 1281.
 Lambert, D. L., & McWilliam, A., 1986, *ApJ*, 304, 436.
 Martic, M., Lebrun, J. C., Appourchaux, T., & Schmitt, J., 2004, In *SOHO 14/GONG 2004 Workshop, Helio- and Asteroseismology: Towards a Golden Future*, ESA SP-559, page 563. arXiv:astro-ph/0409126.
 Mosser, B., Bouchy, F., Catala, C., Michel, E., Samadi, R., Thévenin, F., Eggenberger, P., Sosnowska, D., Moutou, C., & Baglin, A., 2005, *A&A*, 431, L13.
 Nissen, P. E., Hoeg, E., & Schuster, W. J., 1997, In Battrick, B., editor, *Hipparcos Venice '97 Symposium*, page 225. ESA SP-402. <http://astro.estec.esa.nl/SA-general/Projects/Hipparcos/venice.html>.
 Pijpers, F. P., Teixeira, T. C., Garcia, P. J., Cunha, M. S., Monteiro, M. J. P. F. G., & Christensen-Dalsgaard, J., 2003, *A&A*, 406, L15.
 Samadi, R., Goupil, M.-J., Alecian, E., Baudin, F., Georgobiani, D., Trampedach, R., Stein, R., & Nordlund, Å., 2005, *JA&A*, 26, 171.
 Spergel, D. N., Verde, L., Peiris, H. V., Komatsu, E., Nolte, M. R., Bennett, C. L., Halpern, M., Hinshaw, G., Jarosik, N., Kogut, A., Limon, M., Meyer, S. S., Page, L., Tucker, G. S., Weiland, J. L., Wollack, E., & Wright, E. L., 2003, *ApJS*, 148, 175.
 Thévenin, F., Kervella, P., Pichon, B., Morel, P., di Folco, E., & Lebreton, Y., 2005, *A&A*, 436, 253.

TABLE 1
PARAMETERS FOR ν IND (ASSUMING $Z = 0.001$ AND $\alpha = 1.8 \pm 0.1$)

$\Delta\nu$ (μHz)	24.25	\pm	0.25	(1.0%)
T_{eff} (K)	5291	\pm	34	(0.64%)
M (M_{\odot})	0.847	\pm	0.043	(5.1%)
Age (Gyr)	11.4	\pm	2.4	(21%)
L (L_{\odot})	6.21	\pm	0.23	(3.7%)
R (R_{\odot})	2.97	\pm	0.05	(1.7%)
$\log(g/\text{cm s}^{-2})$	3.421	\pm	0.016	(3.8% in g)
angular diameter (mas)	0.956	\pm	0.023	(2.4%)

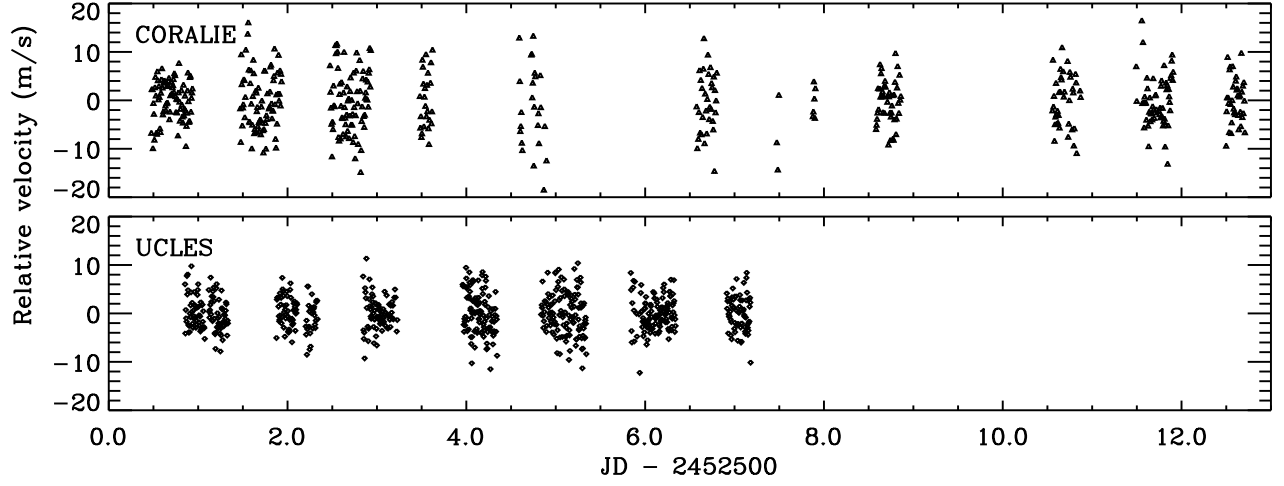


FIG. 1.— Time series of velocity measurements of ν Indi from the UCLES and CORALIE spectrographs. The mean of each night has been subtracted.

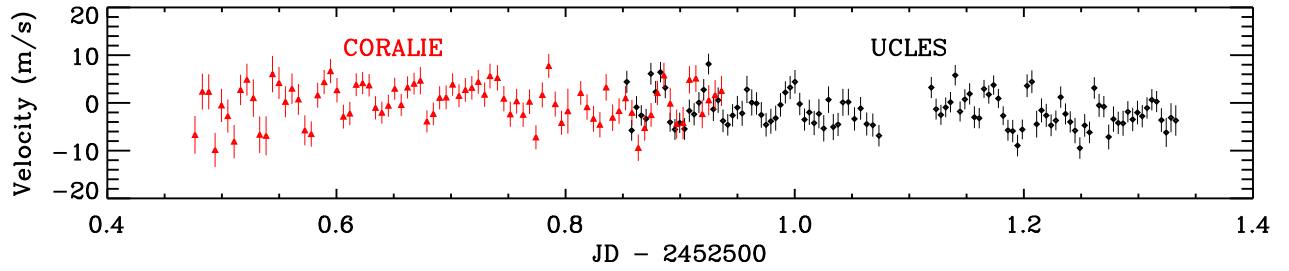


FIG. 2.— Velocities with $1\text{-}\sigma$ error bars for the first night at each site. The 50-minute oscillations are clearly seen.

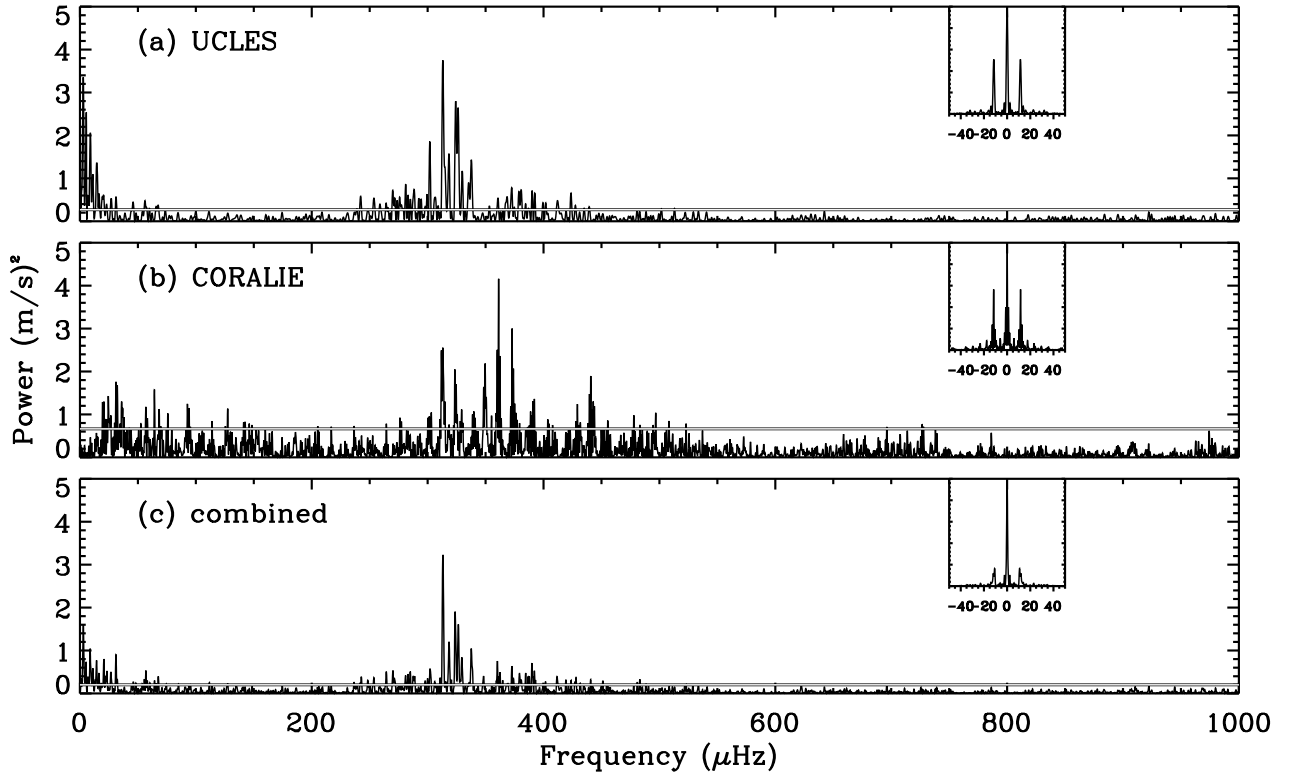


FIG. 3.— Power spectra of velocity measurements of ν Indi from the two time series and from the combined data. The horizontal lines show $(3\sigma)^2$, where σ is the noise at high frequencies in each amplitude spectrum. The inset in each panel shows the spectral window.

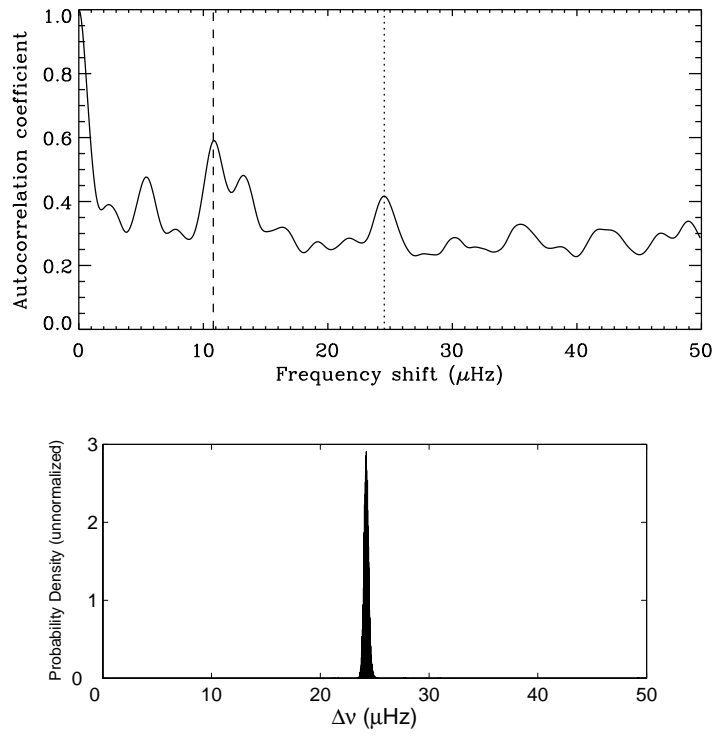


FIG. 4.— Measurements of the large separation of ν Ind. Upper panel: the autocorrelation of the power spectrum, with peaks at $24.5 \mu\text{Hz}$ (dotted line) from the large separation and at $10.8 \mu\text{Hz}$ (dashed line) from the daily sidelobes. Lower panel: probability distribution for the large separation calculated using Bayesian methods (see text).

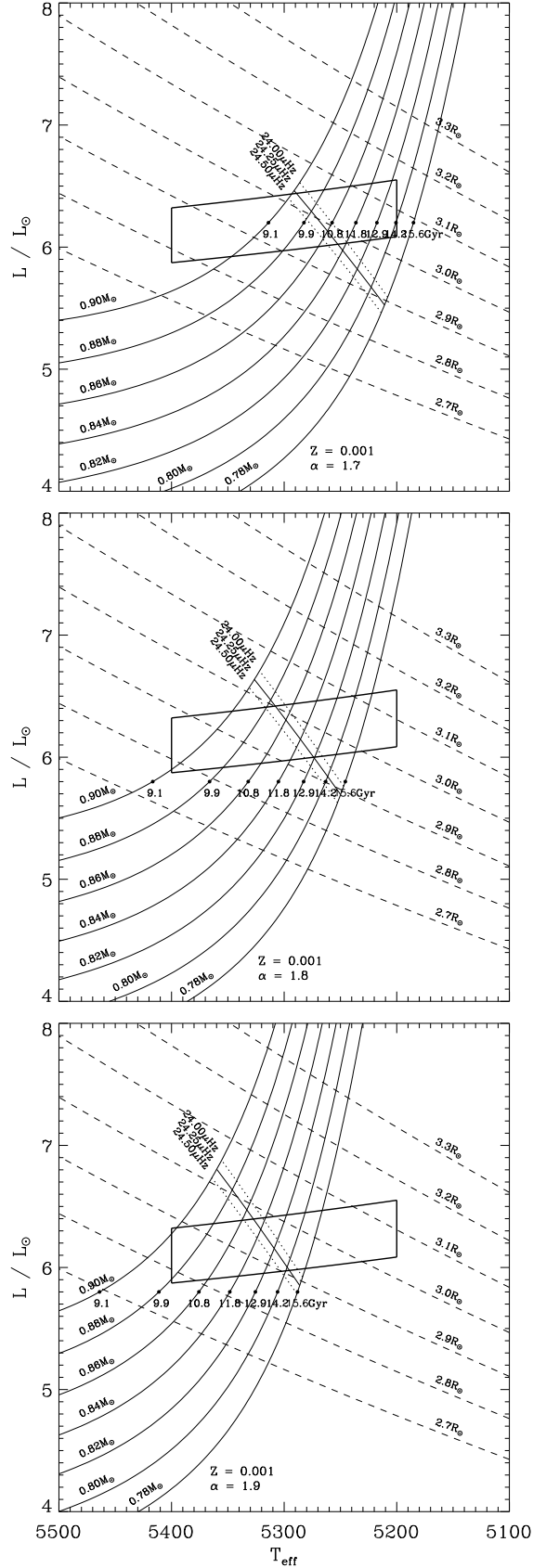


FIG. 5.— H-R diagrams in which the box shows the position of ν Indi from classical observations and the diagonal dashed lines are loci of constant radius. The curved lines are evolutionary tracks for models with $Z = 0.001$ and a range of masses, with the three panels differing in the value of the mixing-length parameter, α . The diagonal lines are loci of constant $\Delta\nu$, calculated from the mean densities of the models by scaling from the Sun.

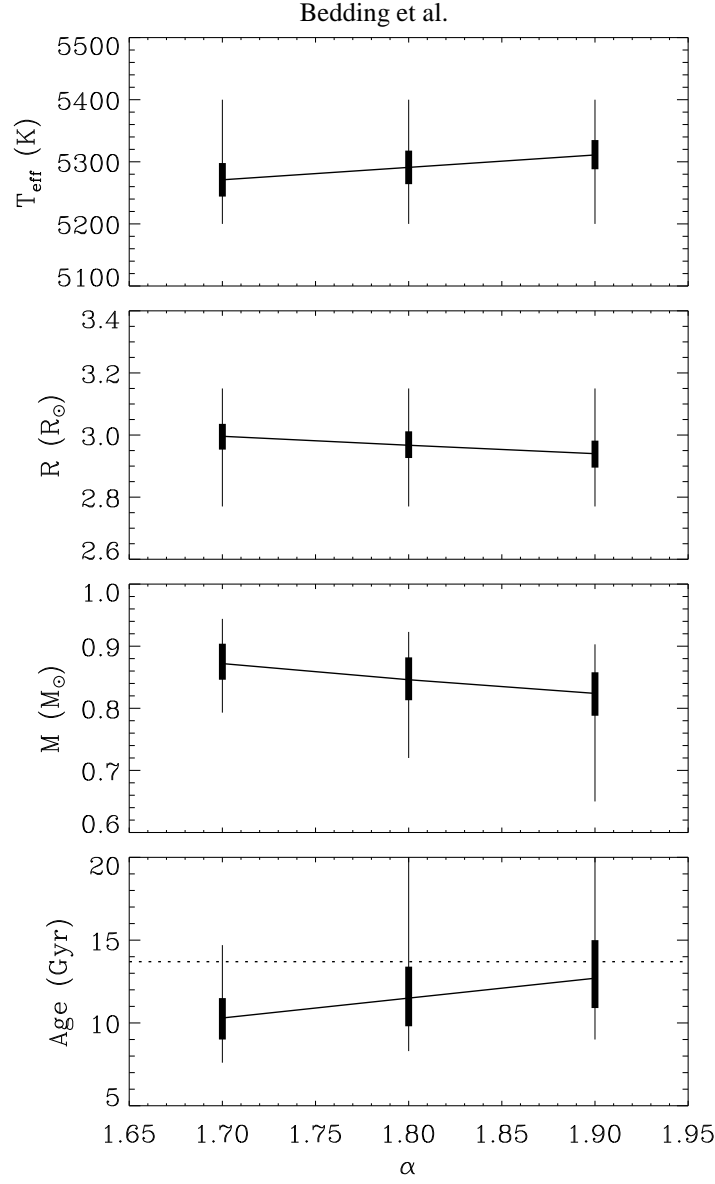


FIG. 6.— Parameters of ν Ind based on observations and models, as a function of the mixing-length parameter. The thin error bars show the range of each parameter based on classical measurements alone (L and T_{eff}), while the thick bars include the constraint provided by our measurement of $\Delta\nu$. The dashed line at an age of 13.7 Gyr indicates the upper limit set by age of the universe (Spergel et al. 2003).

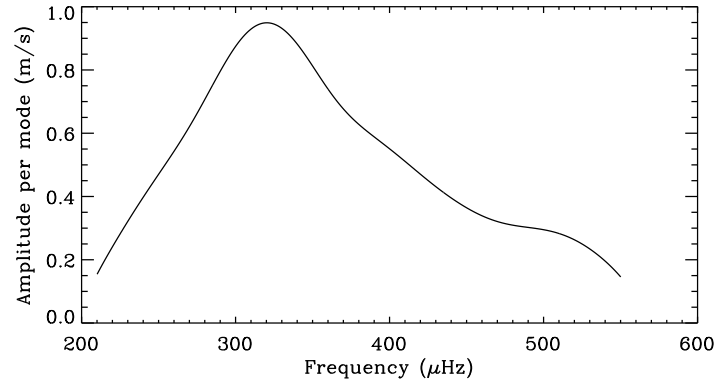


FIG. 7.— Smoothed oscillation spectrum of ν Ind, showing the amplitude per oscillation mode.